OPEN BIOLOGY

royalsocietypublishing.org/journal/rsob

Research

Cite this article: Wimalasiri-Yapa BMCR *et al*. 2021 Temperature modulates immune gene expression in mosquitoes during arbovirus infection. *Open Biol.* **11**: 200246. https://doi.org/10.1098/rsob.20.0246

Received: 12 August 2020
Accepted: 4 December 2020

Subject Area:
microbiology/molecular biology/immunology/genomics

Keywords:
Aedes aegypti, transcriptome, temperature, chikungunya virus, immune genes, RNA seq

Author for correspondence:
Francesca D. Frentiu
e-mail: francesca.frentiu@qut.edu.au

Electronic supplementary material is available online at https://doi.org/10.6084/m9.figshare.c.5238498.

THE ROYAL SOCIETY PUBLISHING

Temperature modulates immune gene expression in mosquitoes during arbovirus infection

B. M. C. Randika Wimalasiri-Yapa[1,4], Roberto A. Barrero[2], Liesel Stassen[1], Louise M. Hafner[1], Elizabeth A. McGraw[5], Alyssa T. Pyke[6], Cassie C. Jansen[7], Andreas Suhrbier[8], Laith Yakob[9], Wenbiao Hu[3], Gregor J. Devine[10] and Francesca D. Frentiu[1]

[1]Institute of Health and Biomedical Innovation, and School of Biomedical Sciences, Faculty of Health, [2]eResearch Office, Division of Research and Innovation, and [3]School of Public Health and Social Work, Queensland University of Technology, Brisbane, Queensland, Australia
[4]Department of Medical Laboratory Sciences, Faculty of Health Science, Open University of Sri Lanka, Nugegoda, Colombo, Sri Lanka
[5]Center for Infectious Disease Dynamics, Department of Entomology, The Pennsylvania State University, University Park, PA 16801, USA
[6]Public Health Virology Laboratory, Forensic and Scientific Services, Coopers Plains, Queensland, Australia
[7]Communicable Diseases Branch, Department of Health, Queensland Government, Herston, Queensland, Australia
[8]Inflammation Biology, QIMR Berghofer Medical Research Institute, Brisbane, Queensland 4006, Australia
[9]London School of Hygiene and Tropical Medicine, London, UK
[10]Mosquito Control Laboratory, QIMR Berghofer Medical Research Institute, Brisbane, Queensland, Australia

BMCRW-Y, 0000-0001-8502-6952; RAB, 0000-0002-7735-665X; LMH, 0000-0002-2117-4945; EAM, 0000-0001-7973-088X; ATP, 0000-0003-3512-4321; AS, 0000-0001-8986-9025; LY, 0000-0001-8639-4511; WH, 0000-0001-6422-9240; GJD, 0000-0001-6312-0390; FDF, 0000-0001-8628-4216

The principal vector of dengue, Zika and chikungunya viruses is the mosquito *Aedes aegypti*, with its ability to transmit pathogens influenced by ambient temperature. We use chikungunya virus (CHIKV) to understand how the mosquito transcriptome responds to arbovirus infection at different ambient temperatures. We exposed CHIKV-infected mosquitoes to 18, 28 and 32°C, and found that higher temperature correlated with higher virus levels, particularly at 3 days post infection, but lower temperature resulted in reduced virus levels. RNAseq analysis indicated significantly altered gene expression levels in CHIKV infection. The highest number of significantly differentially expressed genes was observed at 28°C, with a more muted effect at the other temperatures. At the higher temperature, the expression of many classical immune genes, including *Dicer-2*, was not substantially altered in response to CHIKV. The upregulation of Toll, IMD and JAK-STAT pathways was only observed at 28°C. Functional annotations suggested that genes in immune response and metabolic pathways related to energy supply and DNA replication were involved in temperature-dependent changes. Time post infection also led to substantially different gene expression profiles, and this varied with temperature. In conclusion, temperature significantly modulates mosquito gene expression in response to infection, potentially leading to impairment of immune defences at higher temperatures.

1. Introduction

Arthropod-borne diseases constitute a significant proportion of the global infectious disease burden, with yearly estimates of approximately 1 billion infections and 1 million deaths [1]. Dengue viruses (DENVs 1–4), Zika virus (ZIKV) and chikungunya (CHIKV) are some of the most common pathogens

causing epidemics of arthropod-borne virus (arboviruses) disease in recent decades [2]. These viruses are principally vectored to humans by the mosquitoes *Aedes* (*Ae.*) *aegypti* and *Ae. albopictus* [3]. Because mosquitoes are poikilothermic, almost all their biological activities are influenced by ambient environmental conditions [4], such as temperature. Understanding how mosquitoes respond to changes in this key parameter, over the short and long term, are necessary to improve predictions of arbovirus futures.

Recent projections have suggested that climate change may increase the risk of arbovirus transmission, as higher average temperatures are projected to expand the geographical distributions and lengthen active seasons of arthropod vectors [5–9]. Temperature is also known to alter the ability of *Aedes* spp. mosquitoes to transmit viruses, with higher temperatures following infection leading to increased viral replication and earlier transmission potential [10,11]. Conversely, lower ambient temperatures lead to decreased viral replication and delayed transmission by mosquitoes [12,13]. Exactly how ambient temperature influences the physiological, molecular and genetic interactions between virus and mosquito during infection remains poorly elucidated.

Mosquitoes possess physical and physiological barriers against pathogen infection. Insect protection relies on the humoral and cellular immune responses, which comprise the innate immune system [14]. Mosquito immune response can be divided into four components: pathogen recognition, activation of immune signalling, immune effector mechanisms [15] and immune modulation by the regulation of mosquito homeostasis. Apart from known (termed 'classical') immune genes within these four categories, recent studies have indicated the involvement of additional gene families during arbovirus infection in *Ae. aegypti*. Additional genes included cytoskeleton and cellular trafficking, heat shock response, cytochrome P450, cell proliferation, chitin and small RNAs [15]. Long non-coding RNAs (lncRNAs) are also involved in *Ae. aegypti*–virus interactions, particularly in DENV and ZIKV infections [16,17].

A recent study characterizing the effects of temperature on the flavivirus ZIKV, in *Ae. aegypti* indicated that lower ambient temperature (20°C) leads to a substantially different gene expression profile compared with the predicted optimum temperature for ZIKV transmission (28°C), in the early phase of infection [18]. The same study showed far fewer differences in gene expression in mosquitoes maintained at 28°C versus the higher temperature of 36°C. What is not well understood is whether the patterns observed for ZIKV hold across other arboviruses. Even less well understood is how the mosquito immune response may change in response to temperature during prolonged virus infection, and how this may impact on the insect's ability to vector pathogens.

CHIKV is an emerging arbovirus from the *Alphavirus* genus in the *Togaviridae* family, and is responsible for several recent large outbreaks globally with an estimated 10 million cases [19–21]. Rarely fatal, CHIKV typically causes an acute febrile syndrome and severe, debilitating rheumatic disorders in humans that may persist for months [20,21]. The main vector of CHIKV is *Ae. aegypti* [22], with *Ae. albopictus* also playing an important role in more recent outbreaks [23]. CHIKV cases were reported from Africa, Asia, Europe, and islands of Indian and Pacific Oceans until 2013, when the first autochthonous cases were reported in the Americas on islands in the Caribbean. By the end of 2017, more than 2.6 million suspected cases of CHIKV had been reported from the Caribbean and the Americas [24]. Since then, the virus has continued to circulate and cause sporadic disease and periodic outbreaks with very high attack rates in many areas of the world [24]. CHIKV is a single-stranded, positive sense RNA virus. To date, the interactions between emerging alphaviruses, such as CHIKV, and their mosquito hosts under different temperatures have been less characterized than those of flaviviruses, namely DENV and ZIKV. In addition, although mosquitoes remain infected with arboviruses for life [25], the immune responses underlying long-term persistence of these pathogens is not well understood.

Here, we report how exposure to three ambient temperature regimes (18°C, 28°C and 32°C) alters gene expression in mosquitoes infected with CHIKV, sampled at two time points post infection. We found that temperature alters the transcriptome, with the highest number of upregulated genes observed at 28°C, while lower temperatures were associated with more downregulated genes. Importantly, we observed the absence of *Dicer-2* and low levels of immune gene expression at 32°C, suggesting heat may impair mosquito immunity and the ability to mount an adequate RNAi response. We also show that mosquito gene expression is not constant over the course of arbovirus infection, with distinct gene expression profiles observed for each temperature and time point sampled.

2. Results

2.1. CHIKV replication varies with ambient temperature and time post infection

To determine how ambient temperature modulates replication of CHIKV, and how this may vary over the course of infection, *Ae. aegypti* mosquitoes were orally infected with a CHIKV strain from the Asian genotype (GenBank accession MF773560) and held at 18, 28 or 32°C for either 3- or 7-days post infection (dpi) ($n = 18$–20 mosquitoes per combination of T°C and dpi). Using qRT-PCR (as per [13]), we found that at 3 dpi, the number of virus genome copies in mosquito bodies (including heads but without wings and legs) held at 32°C was significantly higher than that from mosquitoes held at the other temperatures (figure 1*a*). By contrast, at 7 dpi, the highest amount of virus was present in mosquitoes held at 28°C, with a decline in CHIKV copy number observed at 32°C (figure 1*b*). Next, we performed RNAseq on a subset of six mosquitoes for each temperature and time point ($n = 72$ total). Of the 2 661 279 246 Illumina paired end reads generated in this study, 10 155 660 (0.38%) of reads mapped onto the CHIKV genome (MF773560 strain). CHIKV reads obtained from the RNAseq data were largely congruent with qRT-PCR results (figure 1*c*), with the highest read count (normalized reads per million) observed in mosquitoes held at 32°C and sampled at 3 dpi. Normalized viral read counts were significantly correlated with copy number from qRT-PCR ($r^2 = 0.8916$, $p < 0.001$). Two samples, from a total of 72 submitted for RNAseq, were removed from downstream analyses of differential gene expression. These samples were identified as outliers in the correlation between virus titre and normalized read counts (figure 1*c*).

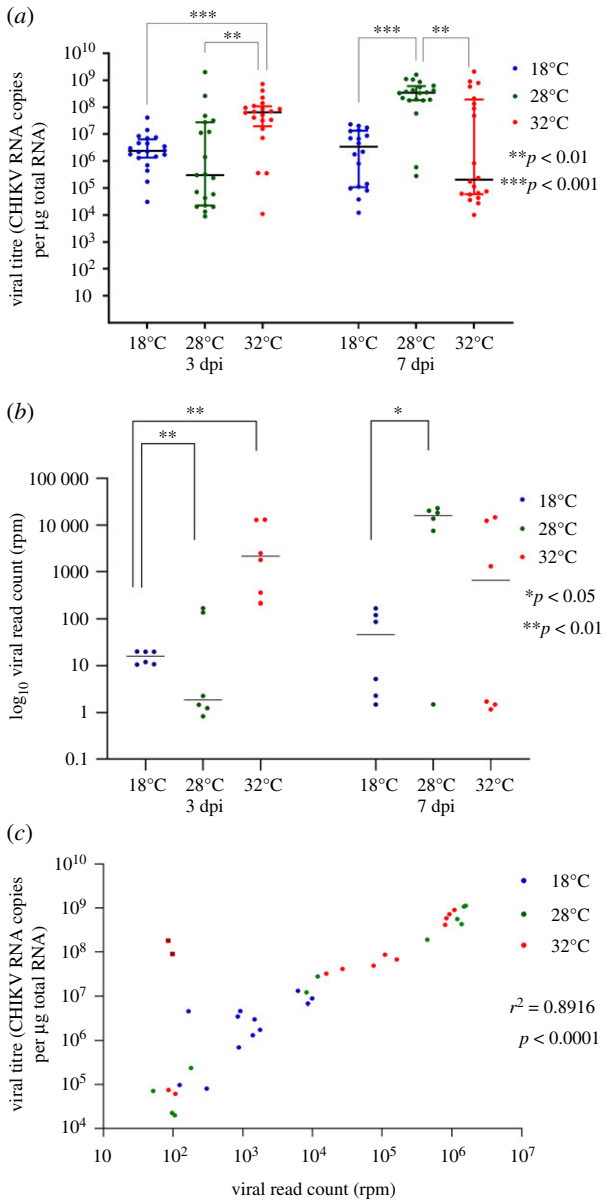

Figure 1. Effect of temperature and day post infection (dpi) on CHIKV replication in *Ae. aegypti* mosquitoes. (*a*) CHIKV RNA copy numbers detected using qRT-PCR in whole mosquito bodies, 18°C ($n = 20$ and $n = 18$), 28°C ($n = 19$ and $n = 20$) and 32°C ($n = 20$ in each time point), sampled at 3 and 7 dpi. Statistical significance was assessed using Mann–Whitney tests. (*b*) CHIKV read counts obtained from RNAseq of *Ae. aegypti* samples (six mosquito bodies per each temperature/dpi combination). Log_{10} normalized reads per million (RPM) counts shown. (*c*) Pearson correlation between body CHIKV titre from qRT-PCR and virus read counts, across all temperatures and both time points. Each point on the plots represents an individual mosquito. The dark blue squares in (*c*) indicate two outlier samples that were removed from downstream analyses of the mosquito transcriptome.

2.2. Temperature alters differential gene expression during CHIKV infection

A total of 2 511 065 774 (94.36%) reads from 70 samples were mapped to the reference genome of *Ae. aegypti*, version AaegL5.2 (electronic supplementary material, table S1). For each temperature and time regime, differentially expressed genes (DEGs) in response to CHIKV infection were identified using DEseq2 by comparison with uninfected control mosquitoes. DEGs were considered statistically significant if the adjusted p-value < 0.05 and absolute fold change (FC) > ± 1.5. At 3 dpi, we detected 715 DEGs across all temperature regimes. We observed a large number of upregulated genes ($n = 374$) in mosquitoes held at 28°C, but a dramatically lower number at 32°C, with classical immune gene expression generally following the same pattern (figure 2*a*; electronic supplementary material, table S2 for a list of genes). At 7 dpi, we found a similar number of DEGs ($n = 726$) in response to CHIKV infection to that observed at 3 dpi (figure 2*b*). The highest number of DEGs was observed in mosquitoes held at 28°C, including classical immune response genes, a pattern similar to 3 dpi (electronic supplementary material, table S3). By contrast, at 7 dpi we observed a substantial decrease in DEGs at 18°C but a marked increase in upregulated DEGs at 32°C.

Volcano plots combining individual mosquito-level variation in gene expression of infected versus uninfected mosquitoes at different temperatures also confirm the observation of a higher number of upregulated than downregulated genes at both 3 (electronic supplementary material, figure S1A–C) and 7 dpi (electronic supplementary material, figure S2A–C). Moreover, heat maps of individual level variation in the gene expression show mosquitoes to be clustered consistently within their infection status (electronic supplementary material, figures S1D–F and S2D–F). To assess the global gene expression profiles in both infected and uninfected mosquitoes, we ran a principal component analysis (PCA) at each tested temperature, at both 3 and 7 dpi (electronic supplementary material, figure S3). PCA plots showed consistent separation of CHIKV-infected and non-infected individual mosquitoes, indicating that observed gene expression changes are consistent across the six biological replicates samples tested for each condition.

Across all temperatures and time points, the top 10 upregulated (in terms of fold change) DEGs were predominantly genes known to be involved in thermoregulatory responses, such as heat shock proteins (particularly *hsp70*) and lethal (2) essential for life protein (*l2efl*) (table 1). By contrast, the top 10 downregulated DEGs were more heterogeneous across all temperatures and both time points. At 3 dpi, proteolysis, intracellular signal transduction, protein-binding and oxidation–reduction process-related genes were among the top 10 downregulated genes at 18°C. At 28°C, downregulated genes were predominantly involved in oxidation-reduction, cell division, zinc ion binding, nucleic acid binding and integral component of membrane (table 1). Four genes downregulated at 32°C were related to oxidation–reduction and protein binding. At 7 dpi, RNA binding, pigment binding, lipid binding and transport, proteolysis and integral component of membrane gene were among the top 10 downregulated genes at 18°C (table 1). Microtubule binding, catalytic activity, odorant binding, membrane and ionotropic glutamate receptor activity genes were among the most downregulated DEGs at 28°C, while odorant binding, nucleotide binding, ATP binding, phototransduction and transferase genes were downregulated at 32°C. Across all temperature regimes and dpi, we observed 11 lncRNAs being among the top 10 downregulated, but no lncRNAs were present among the top 10 upregulated genes (table 1). At 3 dpi, 14 genes were upregulated under all three temperature regimes in response to CHIKV infection, and comprised 10 HSPs, nucleic acid binding and genes involved in regulation of cell cycle (table 2). By 7 dpi, 22 genes that were upregulated across all temperature regimes (table 2) with a similar pattern observed in the categories of genes involved. There were no

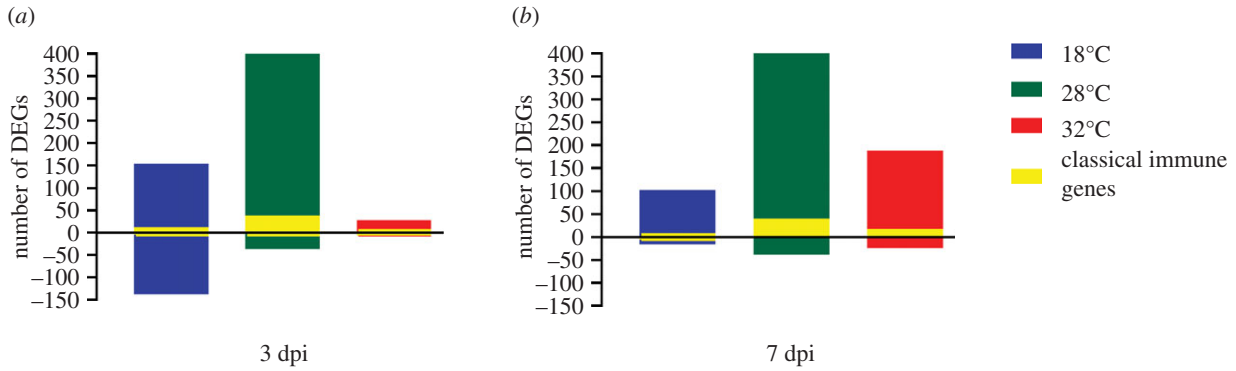

Figure 2. Differentially expressed genes (DEGs) in response to CHIKV infection in *Ae. aegypti*. Mosquitoes were held at three ambient temperatures and sampled at (*a*) 3 dpi and (*b*) 7 dpi. DEGs were identified using DESeq2, with a fold change (FC) > ±1.5 and adjusted *p*-value < 0.05. The number of DEGs involved in the classical immune response is shown in yellow.

downregulated DEGs in common across the three temperatures, for either time points. Overall, the results indicate similar categories of upregulated genes, but far greater heterogeneity of downregulated DEGs, among the temperature regimes in response to CHIKV infection.

2.3. Identification of *Ae. aegypti* genes involved in classical and non-classical immune response and updating annotations of AaegL5.2

To determine how the expression of known mosquito immune genes changes with temperature in response to CHIKV infection, we first identified from ImmunoDB database 445 genes listed under 27 families that were similarly annotated in AaegL1 and AaegL5.2. This indicated that 166 genes were no longer available with the same gene ID in the latest genome annotation release AaegL5.2. Since the release of AaegL1, a number of additional genes have been identified to be involved in mosquito immune response. Using a literature review, we identified 10 additional gene families, resulting in a total of 37 gene families implicated in mosquito immunity (electronic supplementary material, table S4), producing a final list of 998 genes. The list was divided into classical or non-classical components (electronic supplementary material, tables S5 and S6) [26–35]. Genes already identified and directly involved in humoral and cellular immune response were considered as classical immune genes [36]. Genes outside of these classical immune pathways that are transcriptionally altered in response to arboviral infections in *Ae. aegypti* were considered as non-classical immune genes [37]. We next considered DEG patterns in classical immune genes, categorized under the four main processes of immune response: pathogen recognition, immune signalling, pathogen destruction and immune gene modulation.

2.4. Pathogen recognition receptor genes

At both time points sampled post CHIKV infection, the majority of PRR DEGs were observed in mosquitoes held at 28°C (n DEGs = 24; figure 3), with only a handful detected at the other temperatures. The number of PRR DEGs observed at 28°C stayed largely similar at both time points (3 dpi $n = 24$; 7 dpi $n = 30$). Strikingly, only two PRRs were found to be differentially expressed at 32°C at 3 dpi (figure 3*a*), although by 7 dpi that number had increased sixfold (figure 3*b*). By contrast, the number of PRRs differentially expressed at 18°C ($n = 8$) was halved by 7 dpi. PRR DEGs were predominantly CLIP domain serine proteases, leucine-rich immune receptors (LRIM) and leucine-rich repeat-containing proteins (LRR), galectins, fibrinogen-related proteins (FREP), ML/Niemann-pick receptors, peptidoglycan recognition proteins (PGRP), scavenger receptors (SCR) and thioester proteins (TEP). At 3 dpi, two CLIPs (AAEL003632: *CLIPB39*, AAEL012712: *CLIPC13*) and one TEP (AAEL008607: *TEP3*) were found in common to mosquitoes held at 18°C and at 28°C. At 7 dpi, we observed *CLIPD6* (AAEL002124) to be upregulated under all temperatures.

2.5. Immune signalling genes

We found a complete absence of immune signalling DEGs at 32°C at the 3 dpi, with only two DEGs detected by 7 dpi (figure 4). Upregulation of *Cactus* (AAEL000709), *Toll 5A* (AAEL007619) and downregulation of *TRAF6* (AAEL028236) were only found at 18°C (figure 4). *Kayak* (AAEL008953) and *AP-1* (AAEL003505) were expressed at both time points at 18°C and 28°C, but only *AP-1* was observed at 32°C at 7 dpi. The repertoire of immune signalling genes was stable across the two time points at 28°C and included two *Spätzle* genes (AAEL001929 and AAEL013434), *Relish 2* (AAEL007624) gene and a hypothetical protein from JAK-STAT pathway (AAEL009645).

2.6. Pathogen destruction and immune modulation genes

There were no pathogen destruction or related effector DEGs in mosquitoes held at 32°C at 3 dpi, although *Caspase 8* (AAEL014348) was upregulated at 7 dpi (figure 5*a*). *Caspase* 8 and *Dicer-2* (AAEL006794) were upregulated at 18°C at 3 dpi but were not differentially expressed at 7 dpi. Upregulation of *Dicer-2* expression in response to CHIKV was only observed at 18°C and 28°C. By contrast, the mosquitoes kept at 28°C differentially expressed most of the previously identified pathogen destruction mechanisms including antimicrobial peptide (*AMP*) genes (*Attacin*, *Defensin* and *Cecropin*) and apoptosis genes (*Caspase 8* and *IAP 1*). By 7 dpi, most expression of DEGs was suppressed at 18°C and reduced at 28°C. We did not observe any immune modulation genes significantly upregulated at 32°C at 3 dpi, although by 7 dpi two

Table 1. Top 10 differentially expressed genes (DEGs) ranked by fold change in CHIKV-infected *Ae. aegypti* versus uninfected controls, held at three different temperatures (T°C) and sampled at two time points post infection (dpi). L2efl: Lethal (2) essential for life protein, *l2efl*.

		upregulated				downregulated			
dpi	T°C	VectorBase gene ID	gene description	fold change	*p*-adj.	VectorBase Gene ID	gene description	fold change	*p*-adj.
3	18°C	AAEL020330	heat shock protein 70 A1-like	46.38	6.17×10^{-44}	AAEL009165	protein G12	−8.49	6.03×10^{-11}
		AAEL017976	heat shock protein HSP70	38.00	3.82×10^{-42}	AAEL024161	LncRNA	−4.33	2.03×10^{-4}
		AAEL013346	L2efl	35.25	2.98×10^{-37}	AAEL023395	LncRNA	−4.29	5.01×10^{-6}
		AAEL013345	alpha A-crystallin, putative	31.05	2.25×10^{-31}	AAEL012766	cytochrome P450	−4.24	4.53×10^{-7}
		AAEL013350	heat shock protein 26kD, putative	24.42	1.50×10^{-27}	AAEL012717	WD-repeat protein	−3.81	1.42×10^{-3}
		AAEL013348	L2efl	21.51	3.51×10^{-26}	AAEL008609	zinc carboxypeptidase	−3.77	9.81×10^{-7}
		AAEL013339	alpha A-crystallin, putative	19.17	1.59×10^{-21}	AAEL001693	serine-type enodpeptidase	−3.56	9.69×10^{-4}
		AAEL013349	L2efl	15.77	1.58×10^{-20}	AAEL013118	insect allergen-related protein	−3.53	2.61×10^{-3}
		AAEL017975	heat shock protein HSP70	14.48	2.70×10^{-18}	AAEL008701	myoinositol oxygenase	−3.52	2.31×10^{-3}
		AAEL013351	L2efl	14.15	1.89×10^{-25}	AAEL009843	serine-type endopeptidase	−3.51	2.39×10^{-3}
3	28°C	AAEL013350	heat shock protein 26kD, putative	201.82	5.02×10^{-120}	AAEL012628	DNA-binding transcription factor activity	−6.98	1.51×10^{-9}
		AAEL013339	alpha A-crystallin, putative	73.87	2.21×10^{-85}	AAEL000507	chorion peroxidase	−3.94	5.00×10^{-6}
		AAEL020330	heat shock protein 70 A1-like	69.08	9.43×10^{-56}	AAEL018189	PCR Gastrin/Cholecystokinin Family	−3.29	9.96×10^{-4}
		AAEL017976	heat shock protein HSP70	66.81	3.41×10^{-57}	AAEL020175	LncRNA	−3.27	3.58×10^{-3}
		AAEL017975	heat shock protein HSP70	59.88	2.05×10^{-66}	AAEL005507	inhibitory pou (eukaryotic transcription factors containing a bipartite DNA-binding domain referred to as the POU)	−3.26	4.12×10^{-3}
		AAEL013346	L2efl	47.65	1.21×10^{-46}	AAEL009899	uncharacterized LOC5572580, cellular component/membrane/nucleotide binding	−2.87	1.11×10^{-4}
		AAEL022253	pseudogene	28.78	4.88×10^{-35}	AAEL012566	zinc finger C_2H_2-type/integrase DNA-binding domain	−2.75	1.70×10^{-2}
		AAEL013348	L2efl	27.20	1.69×10^{-43}	AAEL010855	cdc6	−2.65	2.37×10^{-3}
		AAEL027610	heat shock protein 70 A1	25.78	3.18×10^{-27}	AAEL022900	LncRNA	−2.58	3.30×10^{-2}
		AAEL024512	pseudogene	13.27	3.61×10^{-30}	AAEL022382	LncRNA	−2.45	3.00×10^{-2}

(*Continued*.)

Table 1. (*Continued.*)

		upregulated				downregulated			
dpi	T°C	VectorBase gene ID	gene description	fold change	*p*-adj.	VectorBase Gene ID	gene description	fold change	*p*-adj.
3	32°C	AAEL013339	alpha A-crystallin, putative	5.61	2.37×10^{-7}	AAEL024207	uncharacterized LOC5568345, binding and developmental process involved in reproduction	−2.97	2.28×10^{-2}
		AAEL013349	L2efl	4.16	2.05×10^{-4}	AAEL014019	cytochrome P450	−2.71	4.47×10^{-2}
		AAEL013346	L2efl	4.07	2.39×10^{-4}	AAEL000668	protein flightless1 homologue	−2.66	4.39×10^{-2}
		AAEL013345	alpha A-crystallin, putative	3.88	4.42×10^{-4}	AAEL011126	alcohol dehydrogenase	−2.42	4.85×10^{-2}
		AAEL017976	heat shock protein HSP70	3.84	4.42×10^{-4}				
		AAEL013348	L2efl	3.71	5.17×10^{-4}				
		AAEL020330	heat shock protein 70 A1-like	3.58	1.55×10^{-3}				
		AAEL013350	heat shock protein 26kD, putative	3.55	1.67×10^{-3}				
		AAEL013351	L2efl	3.10	6.31×10^{-4}				
		AAEL009682	serine collagenase 1 precursor, putative	2.92	2.21×10^{-2}				
7	18°C	AAEL013346	L2efl	18.08	3.46×10^{-39}	AAEL006151	serine protease, putative	−2.83	0.0028558
		AAEL013350	heat shock protein 26kD, putative	14.84	6.50×10^{-30}	AAEL009567	apolipoprotein D, putative	−2.80	0.0028558
		AAEL013339	alpha A-crystallin, putative	13.14	4.79×10^{-28}	AAEL010620	uncharacterized protein C6orf203/RNA binding	−2.44	0.0208878
		AAEL013348	L2efl	11.02	2.72×10^{-31}	AAEL029039	CTLGA4	−2.42	0.0017231
		AAEL013351	L2efl	9.18	1.25×10^{-23}	AAEL008789	apolipophorin-III, putative	−2.39	0.0072375
		AAEL017975	heat shock protein HSP70	8.86	1.58×10^{-18}	AAEL018189	PCR Gastrin/Cholecystokinin Family	−2.36	0.02325
		AAEL017976	heat shock protein HSP70	8.83	6.82×10^{-18}	AAEL025334	alpha-macroglobulin, receptor-binding domain superfamily	−2.31	0.0312282
		AAEL013349	L2efl	5.62	3.75×10^{-11}	AAEL020035	putative uncharacterized protein DDB_G0283431 (LOC110679006)	−2.28	0.0304633
		AAEL022253	pseudogene	5.43	5.03×10^{-10}	AAEL013432	serine protease, putative	−2.06	0.0257032
		AAEL024512	pseudogene	5.23	8.49×10^{-10}	AAEL006377	leucine-rich immune protein (Coil-less)	−1.90	0.0236374

(*Continued.*)

Table 1. (*Continued.*)

		upregulated				downregulated			
dpi	T°C	VectorBase gene ID	gene description	fold change	*p*-adj.	VectorBase Gene ID	gene description	fold change	*p*-adj.
7	28°C	AAEL013350	heat shock protein 26kD, putative	8.67	1.52×10^{-21}	AAEL024284	pseudogene	−2.36	2.75×10^{-3}
		AAEL017975	heat shock protein HSP70	8.43	5.11×10^{-21}	AAEL015566	odorant binding protein OBP62	−2.25	5.62×10^{-3}
		AAEL010434	vitellogenin-A1 precursor	6.21	3.55×10^{-15}	AAEL021449	uncharacterized LOC110681489	−2.18	9.18×10^{-3}
		AAEL020330	heat shock protein 70 A1-like	5.74	1.78×10^{-13}	AAEL024757	ionotropic glutamate receptor	−2.17	9.37×10^{-3}
		AAEL013346	L2efl	5.43	1.17×10^{-12}	AAEL002173	TRAF3-interacting protein 1	−2.10	1.43×10^{-2}
		AAEL025531	glycine-rich protein 5-like	4.95	3.80×10^{-12}	AAEL022124	LncRNA	−2.01	2.09×10^{-2}
		AAEL002655	matrix metalloproteinase	4.91	9.82×10^{-12}	AAEL008454	isochorismatase-like	−1.95	2.41×10^{-2}
		AAEL025126	glycine-rich protein 23-like	4.91	9.82×10^{-12}	AAEL019629	putative leucine-rich repeat-containing protein DDB_G0290503	−1.95	3.32×10^{-2}
		AAEL006883	regulation of cell cycle	4.90	5.40×10^{-18}	AAEL026107	LncRNA	−1.94	2.00×10^{-2}
		AAEL017976	heat shock protein HSP70	4.74	1.12×10^{-10}	AAEL004576	uncharacterized protein family, zinc metallopeptidase-like	−1.92	3.86×10^{-2}
7	32°C	AAEL017976	heat shock protein HSP70	7.57	5.31×10^{-12}	AAEL024449	pseudogene	−3.71	1.09×10^{-4}
		AAEL027610	heat shock protein 70 A1	7.37	1.38×10^{-11}	AAEL018041	UDP-glucuronosyltransferase 1-1-like	−3.26	7.04×10^{-4}
		AAEL017975	heat shock protein HSP70	5.37	6.81×10^{-8}	AAEL006938	serine–tRNA synthetase-like protein Slimp	−3.15	4.13×10^{-4}
		AAEL020330	heat shock protein 70 A1-like	4.83	1.04×10^{-6}	AAEL020306	LncRNA	−2.92	3.57×10^{-3}
		AAEL027829	pancreatic lipase-related protein 2	4.31	3.30×10^{-6}	AAEL024183	LncRNA	−2.87	4.55×10^{-3}
		AAEL014020	uncharacterized LOC5579148	4.28	9.71×10^{-6}	AAEL000035	odorant binding protein (Obp57)	−2.86	4.53×10^{-3}
		AAEL013350	heat shock protein 26kD, putative	4.22	1.25×10^{-5}	AAEL005621	long wavelength-sensitive opsin	−2.82	5.52×10^{-3}
		AAEL003345	argininosuccinate lyase	3.70	1.59×10^{-5}	AAEL023039	LncRNA	−2.43	1.12×10^{-2}
		AAEL022059	pseudogene	3.60	2.08×10^{-4}	AAEL026029	LncRNA	−2.42	1.98×10^{-2}
		AAEL001098	clip-domain serine protease, putative	3.55	1.42×10^{-6}	AAEL022225	uncharacterized LOC5565165	−2.40	2.24×10^{-2}

Table 2. Genes observed to be differentially expressed in common across the three temperatures, in CHIKV-infected *Ae. aegypti* sampled at two time points post infection (dpi).

3 dpi		7 dpi	
gene ID	description	gene ID	description
AAEL020330	heat shock protein 70 A1-like (LOC110674152), mRNA	AAEL013346	Hsp20 domain
AAEL017976	HSP70Bb	AAEL013350	Hsp20 domain
AAEL013346	Hsp20 domain	AAEL017975	heat shock protein HSP70
AAEL013345	Hsp20 domain	AAEL017976	HSP70Bb
AAEL013350	Hsp20 domain	AAEL013347	Hsp20 domain
AAEL013348	Lethal (2) essential for life protein, l2efl	AAEL022079	LncRNA
AAEL013351	Lethal (2) essential for life protein, l2efl	AAEL019751	uncharacterized LOC5571127, mRNA
AAEL013339	alpha A-crystallin, putative	AAEL022253	pseudogene
AAEL013349	Lethal (2) essential for life protein, l2efl	AAEL022059	pseudogene
AAEL023321	heat shock protein 70 A1-like	AAEL027610	heat shock protein 70 A1
AAEL004090	SERAC1	AAEL006883	conserved hypothetical protein, Fox O pathway
AAEL006883	conserved hypothetical protein, Fox O pathway	AAEL026008	uncharacterized LOC110675610
AAEL010068	putative uncharacterized protein DDB_G0277255	AAEL013770	zinc finger protein
AAEL024560	dendritic arbor reduction protein 1	AAEL003505	Jun
		AAEL008622	Jnk
		AAEL003728	uncharacterized LOC5578871
		AAEL023591	Myb-like protein V
		AAEL028247	uncharacterized LOC110678629
		AAEL013341	Lethal (2) essential for life protein, l2efl
		AAEL020330	heat shock protein 70 A1-like
		AAEL013345	alpha A-crystallin, putative
		AAEL002124	CLIPD6

serpins were observed (figure 5*b*). Conversely, we observed three immune modulation DEGs (AAEL003182: *SRPN26*; AAEL010235: allergen; AAEL006347: *apyrase*) downregulated at 18°C at 3 dpi but none at 7 dpi.

2.7. Gene ontology mapping differs across temperature and time

The lists of DEGs identified for each temperature and time point sampled were submitted to the DAVID bioinformatics (V6.8) functional annotation tool. The resulting gene ontology (GO) terms were classified using WEGO 2.0 web gene ontology annotation plotting. Gene ontologies in the three major categories of cellular location, molecular function and biological processes differed according to temperature and time of sampling post infection (figure 6; electronic supplementary material, table S7). At 3 dpi, a total of 14 cellular location terms were obtained from the DEGs identified (figure 6*a* left panel) with the majority being present at 18°C. Consistent with the low number of DEGs found at 32°C, only very few cellular location terms were mapped for this temperature. Only five GO terms pertaining to cellular locations were mapped at all three temperatures. At 7 dpi, a similar number of cellular locations related to DEGs was mapped as for 3 dpi (n locations = 13; figure 6*a*, right panel). The highest number of cellular locations was observed for mosquitoes held at 28°C. At 18°C, almost all (8/9) cellular locations comprised upregulated DEGs. Both 28°C and 32°C were similar with respect to DEG expression. Cell junction, supramolecular complex, synapse and synapse part related genes were upregulated only at 28°C.

At 3 dpi, DEGs were related to a total of 10 molecular functions (figure 6*b*, left panel), with catalytic activity significantly differentially expressed at all temperatures. Six, ten and three molecular functions were differentially expressed at 18°C, 28°C and 32°C respectively. Five out of six molecular functions identified in mosquitoes held at 18°C post infection had significant DEGs (both up and downregulated) while the remaining category, behaviour, was downregulated. Binding was downregulated only at 32°C, but transporter activity was upregulated. Cargo receptor activity, molecular function regulator and nutrient reservoir activity were functions observed only at 28°C. Mosquitoes held at the other two temperatures had no DEGs related to these molecular functions. Structural molecular activity was upregulated at both 18°C and 28°C. At 7 dpi, seven out of nine molecular functions were found in common across all temperatures (figure 6*b*, right panel). Cargo receptor activity was only significantly upregulated at 28°C. Molecular transducer activity was observed to be upregulated at 18°C and 28°C while 32°C observed to be downregulated. Nutrient reservoir activity was upregulated at 28°C and 32°C.

DEGs in CHIKV-infected mosquitoes versus controls sampled at 3 dpi related to 17 biological processes, across the

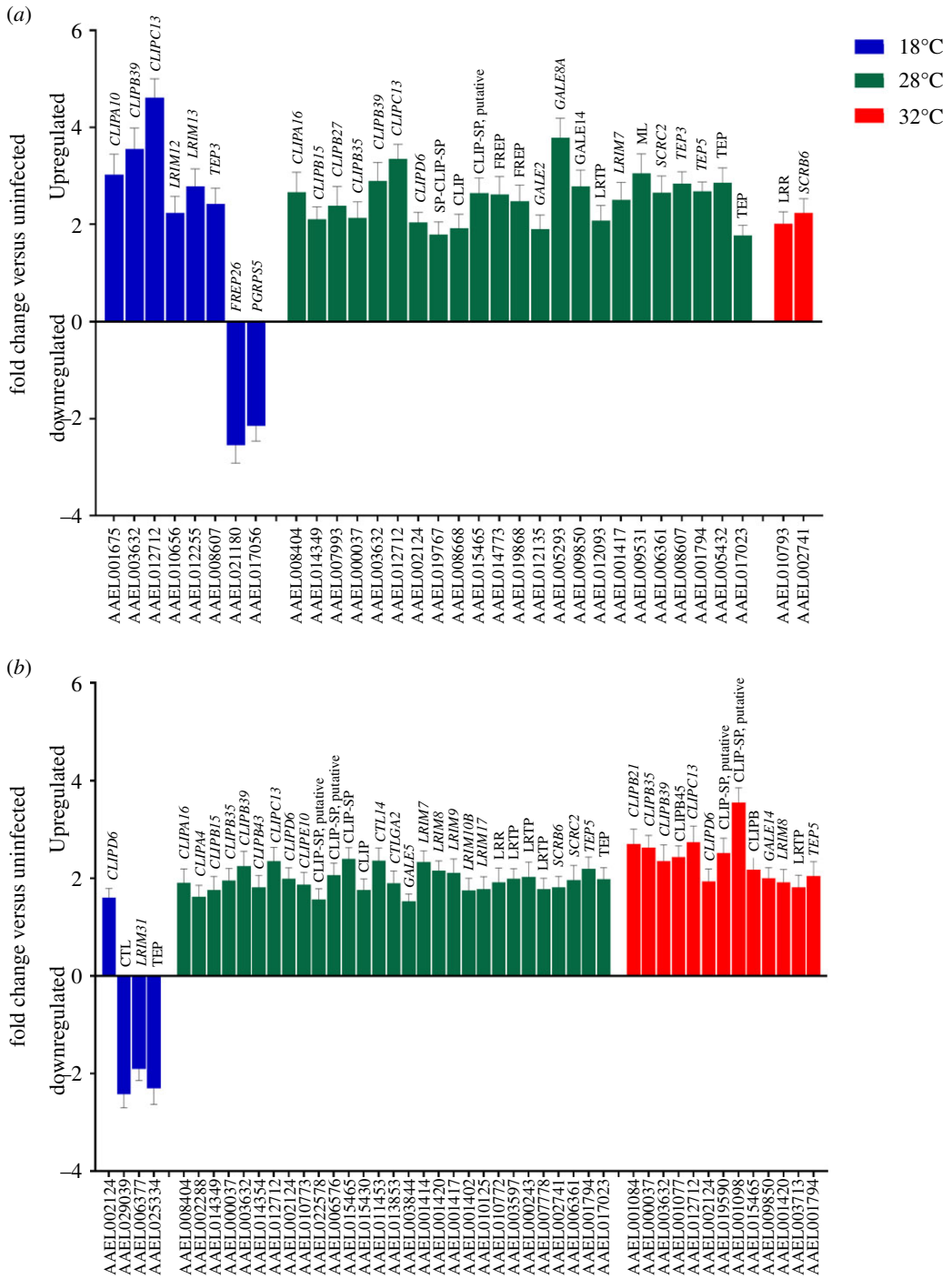

Figure 3. Differentially expressed genes (DEGs) related to pathogen recognition at (*a*) 3 dpi and (*b*) 7 dpi, in CHIKV-infected *Ae. aegypti* versus uninfected controls. CTL: C-type lectin; LRIM: leucine-rich immune receptors; LRR: leucine-rich repeat-containing proteins; LRTP: leucine-rich transmembrane protein; FREP: fibrinogen-related proteins; ML: Niemann-Pick receptors; GALE: galectin; PGRP: peptidoglycan recognition proteins; SCR: scavenger receptors; TEP: thioester proteins. Error bars represent standard error of the mean.

three different temperatures (figure 6*c*, left panel). Mosquitoes from 28°C displayed the highest number (15/17) of differentially expressed biological processes, whereas those kept at 32°C displayed the lowest (5/21). Downregulation of behaviour was unique for mosquitoes held at 18°C. On the other hand, downregulation of cell proliferation and upregulation of cellular component organization of biogenesis and development process were exclusively found at 28°C. Immune system and multicellular organismal processes were downregulated at 18°C but upregulated at 28°C. At 7 dpi, 19 biological functions were identified from DEGs across all temperatures (figure 6*c*, right panel), with the highest number ($n = 18$) identified at 28°C. Upregulation of immune system process and negative regulation of reproduction were exclusively found at 28°C. The majority (6/9) of the biological processes found at 18°C consisted of upregulated DEGs. Further, 62% (8/13) of the biological processes at 32°C were significantly altered through up- and downregulation.

2.8. Impact of temperature on functional pathway enrichment

KEGG pathways obtained from the DAVID Bioinformatics analysis above were manually categorized into KEGG orthologies (groups of pathways) to determine functional

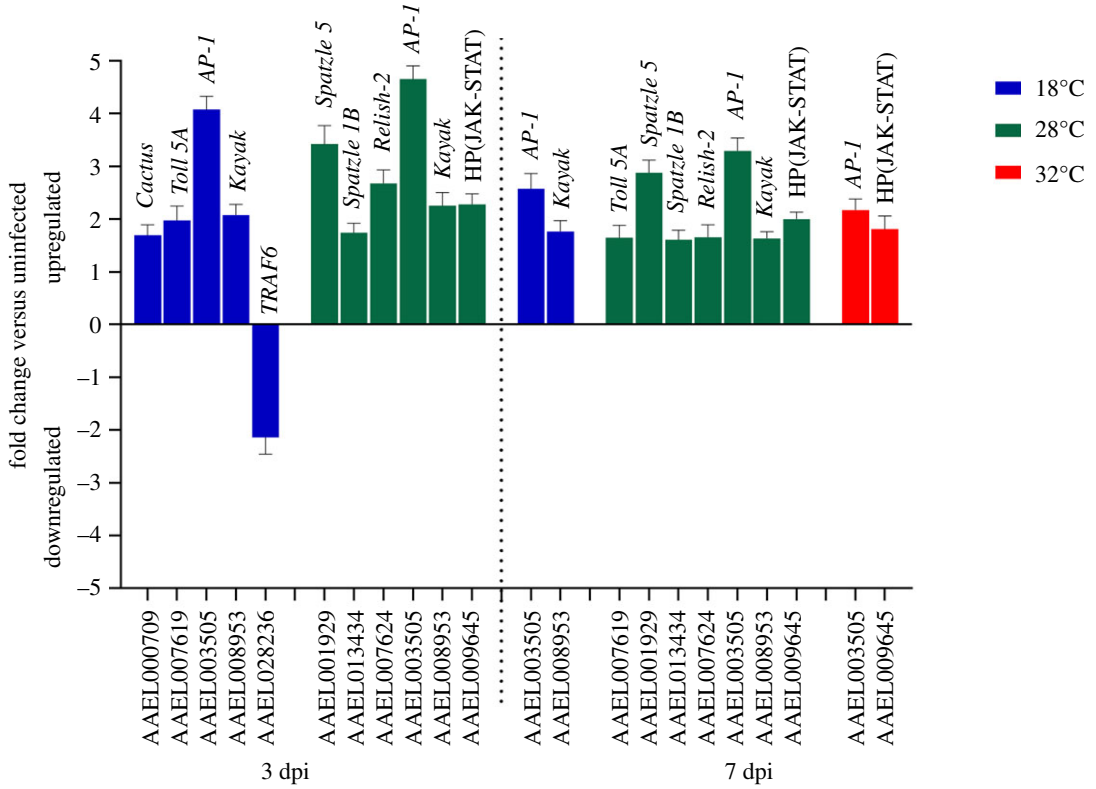

Figure 4. Differentially expressed genes (DEGs) related to immune signalling at (*a*) 3 dpi and (*b*) 7 dpi, in CHIKV-infected *Ae. aegypti* versus uninfected controls. HP indicates hypothetical protein. Error bars represent standard error of the mean.

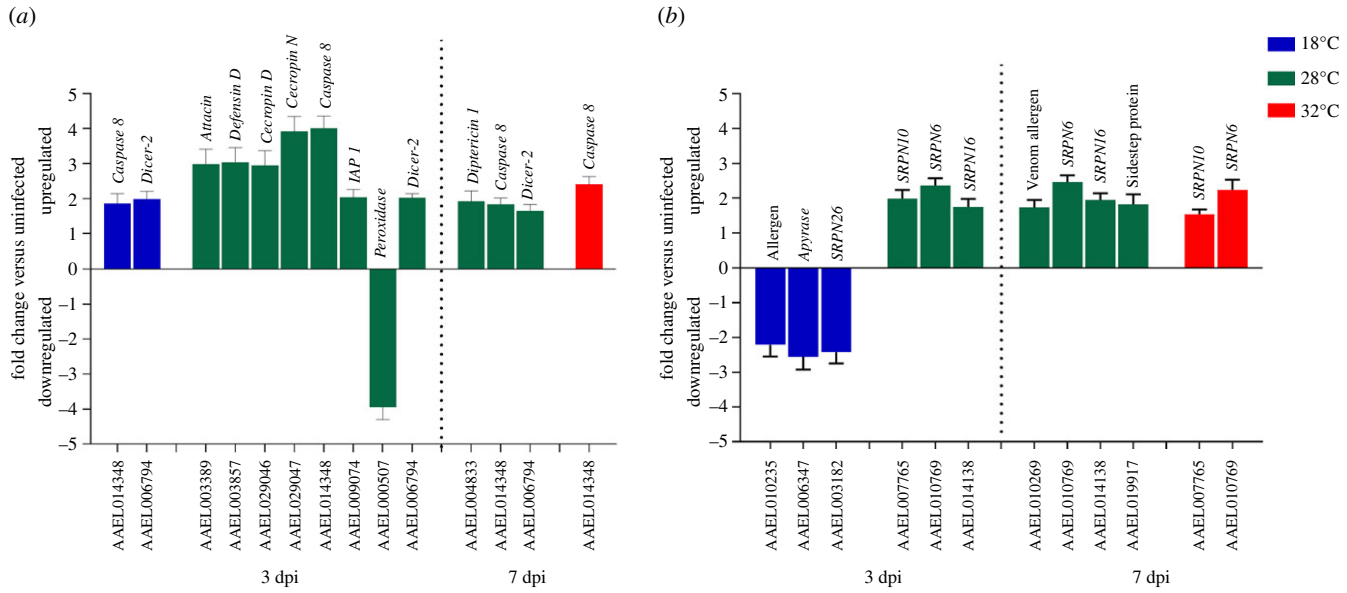

Figure 5. Differentially expressed genes (DEGs) related to (*a*) pathogen destruction and (*b*) immune modulation, in CHIKV-infected *Ae. aegypti* versus uninfected controls sampled at two time points (dpi). SRPN: *serpin*. Error bars represent standard error of the mean.

enrichment. The vast majority of pathways altered by temperature, at both time points, were involved in metabolism (figure 7*a*; electronic supplementary material, table S8). At 3 dpi, 36 metabolic pathways differed significantly between CHIKV-infected and control mosquitoes across all temperatures. The majority of pathways found at 18°C were downregulated, suggesting some degree of metabolic shutdown in infected mosquitoes. Downregulated pathways were mostly related to carbohydrate, amino acid and glycan metabolism (figure 7*a*). At 32°C, all three enriched pathways were downregulated and categorized under metabolic pathways and carbohydrate metabolism. By day 7 post infection, 44 metabolic pathways differed between CHIKV-infected and control mosquitoes. Unlike for 3 dpi, there was no difference in enrichment of metabolic pathways at 18°C between the two mosquito groups. By contrast, 21 pathways were upregulated at 32°C at this time point compared with only three at 3 dpi. A greater number of enriched metabolic pathways was also observed in mosquitoes at 28°C at 7 dpi versus 3 dpi. Ascorbate and aldarate metabolism, glycerophospholipid metabolism and ether lipid metabolism DEGs were only observed at 32°C.

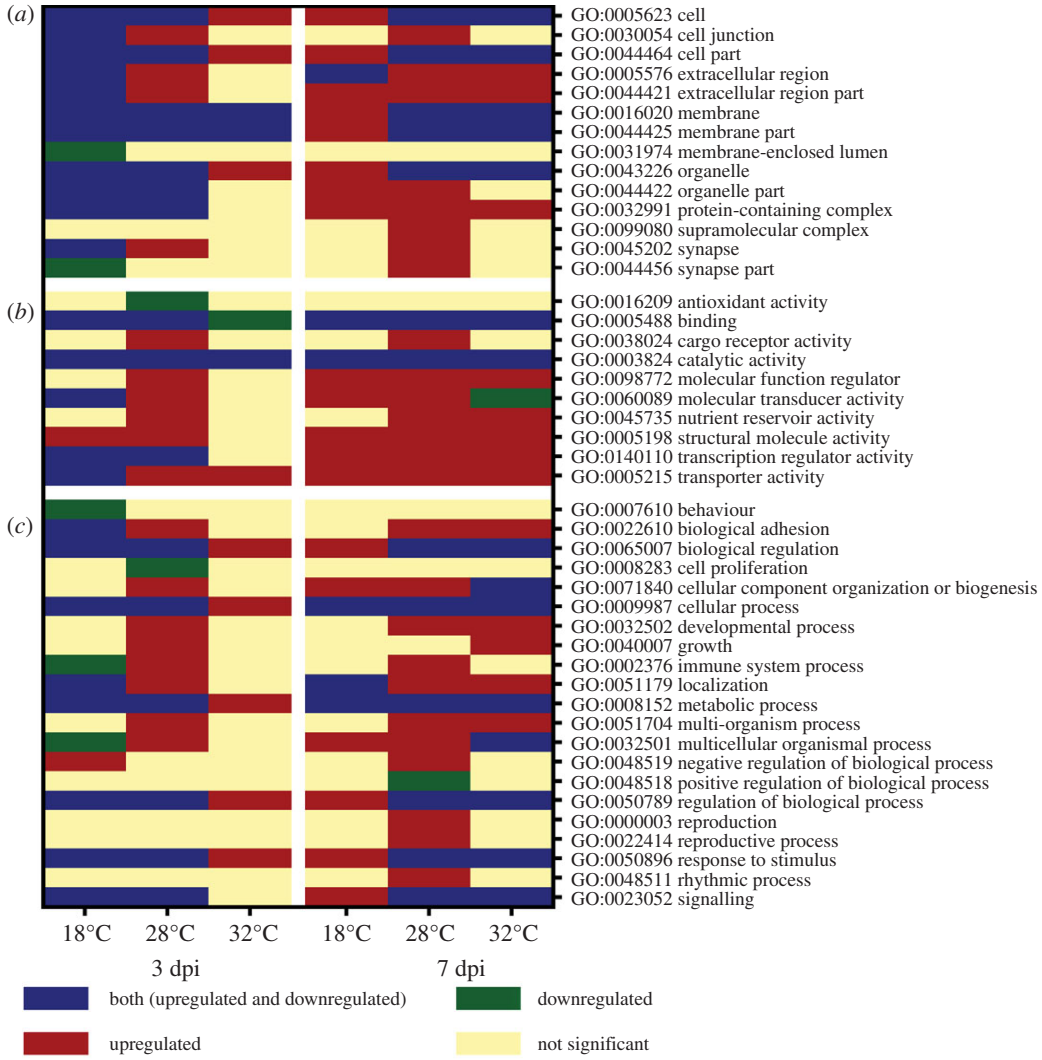

Figure 6. Gene Ontology analysis of differentially expressed genes (DEGs) in CHIKV-infected *Ae. aegypti* mosquitoes, held at three temperatures and sampled at two time points post infection (dpi). (*a*) Cellular locations; (*b*) molecular functions; (*c*) biological processes.

Pathways involved in genetic and environmental information processing and cellular processes also showed enrichment in CHIKV-infected mosquitoes compared with uninfected controls. At 3 dpi, involvement of pathways in these categories was observed only at 18°C and 28°C, with only FoxO signalling present at 32°C. Almost half of the 15 non-metabolic pathways enriched at 18°C were downregulated (figure 7*b–f*). Pathways involved in response to RNA virus infection such as lysosome, phagosome, peroxisome and RNA degradation were significantly downregulated at 18°C but upregulated at 28°C (figure 7*c*,*d*). Some pathways were exclusively differentially expressed at 28°C, including DNA replication, spliceosome, base excision repair, nucleotide excision repair, ABC transporters, Hedgehog pathway, TGF-beta signalling pathway, dorso-ventral axis formation and phototransduction-fly (figure 7*b*,*c*). At 7 dpi, the majority of pathways detected were upregulated (9/10, 10/13 and 9/12 at 18°C, 28°C and 32°C, respectively; figure 7). Upregulation of phagosome and downregulation of endocytosis were exclusively found at 18°C while upregulation of RNA transport and ECM receptor interaction were unique to 28°C. On the other hand, upregulation of mRNA surveillance pathway and regulation of autophagy, but downregulation of aminoacyl tRNA biosynthesis and ubiquitin-mediated proteolysis were distinctly seen at 32°C. Most mosquito groups, except those held at 32°C for 3 dpi, showed enrichment of insulin-resistance pathway.

2.9. Unmapped genes in gene enrichment analysis and long non-coding RNA (lncRNA)

We found 266 upregulated genes and 80 downregulated genes that could not be mapped with DAVID bioinformatics cloud map (figure 8; electronic supplementary material, table S9). Among these, 123 upregulated and 40 downregulated lncRNA genes were found (electronic supplementary material, table S10). That is, on average, nearly 50% of unmapped genes were found to comprise lncRNAs. Overall, 10.32% of all upregulated and 16.06% of all downregulated DEGs were lncRNAs.

3. Discussion

Ambient temperature influences the ability of mosquitoes to transmit viruses but the molecular mechanisms underpinning this are not well understood. Consistent with previous reports, mosquitoes in our experiment that were held at relatively low ambient temperatures showed reduced CHIKV replication.

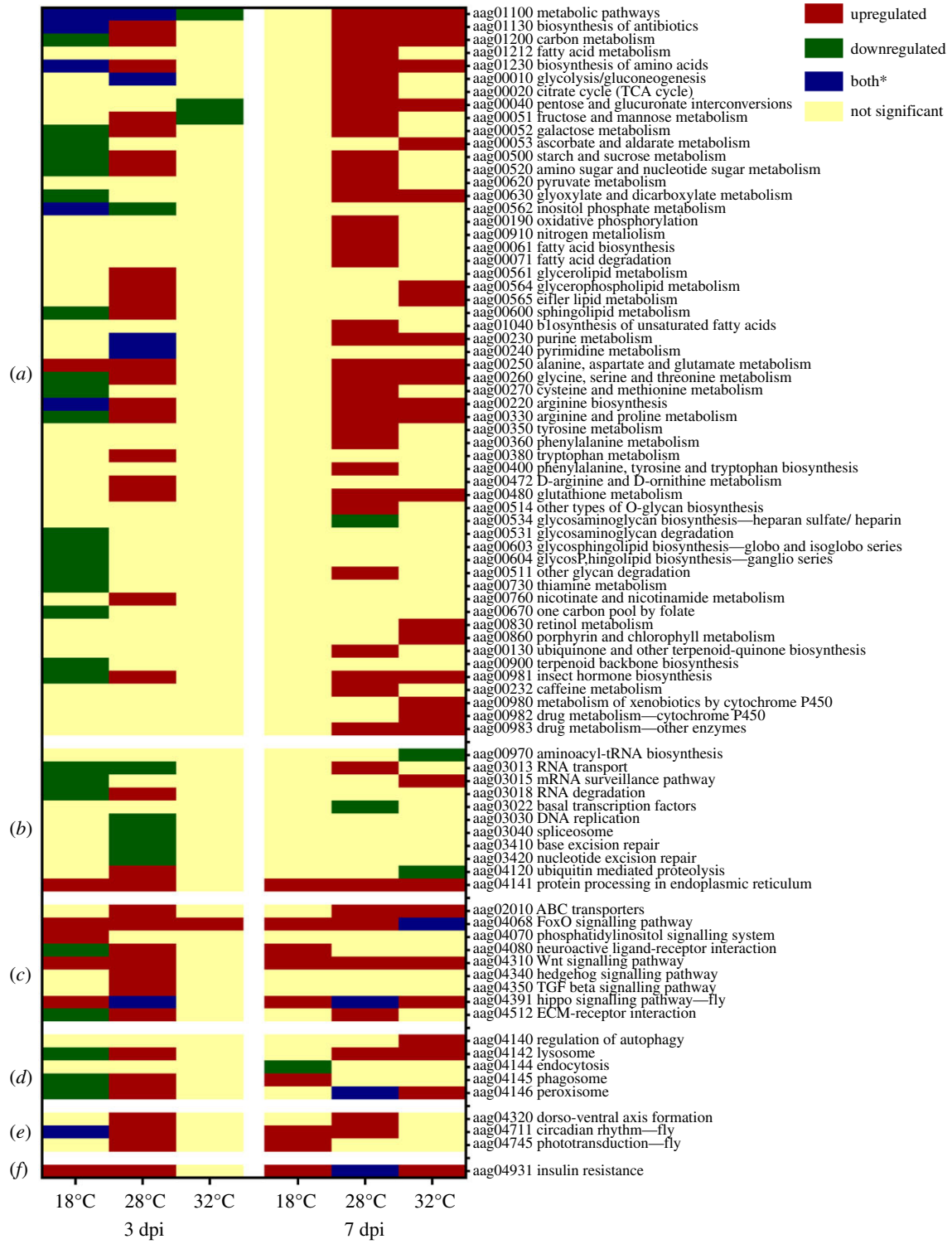

Figure 7. KEGG pathway analysis for DEGs found at 3 dpi and 7 dpi. (*a*) Metabolic pathways; (*b*) genetic information processing; (*c*) environmental information processing; (*d*) cellular processes; (*e*) organismal systems; (*f*) human diseases. 'aag' followed by numbers indicate the KEGG pathway identification number. *Denotes both upregulated and downregulated components to the pathway.

Correspondingly, we observed increased replication at 3 dpi at the highest temperature used here. Higher temperatures increase metabolic rates [38] and thus increase energy production or accumulation of resources necessary for virus replication, potentially underlying the pattern observed [39]. Distinct mosquito gene expression profiles underpinned infection response at different ambient temperatures, both in the absolute number of DEGs but also their gene identities. Similar to our findings for 28°C, a recent study of mosquitoes held at 30°C found a larger number of DEGs expressed at 3 dpi in response to CHIKV [35]. However, exposure to 32°C in our study elicited a surprisingly low number of genes being expressed in response to CHIKV compared with control uninfected mosquitoes, particularly at the earlier time point. This suppressed response is consistent with increased CHIKV replication at this temperature and suggests that, at high temperatures, mosquitoes are unable to mount an effective defence soon after virus infection.

We observed that the repertoire of immune genes differentially expressed in response to CHIKV infection differed across all temperatures at each time point, contrary to what might have been expected [16,40]. The first step in eliciting an

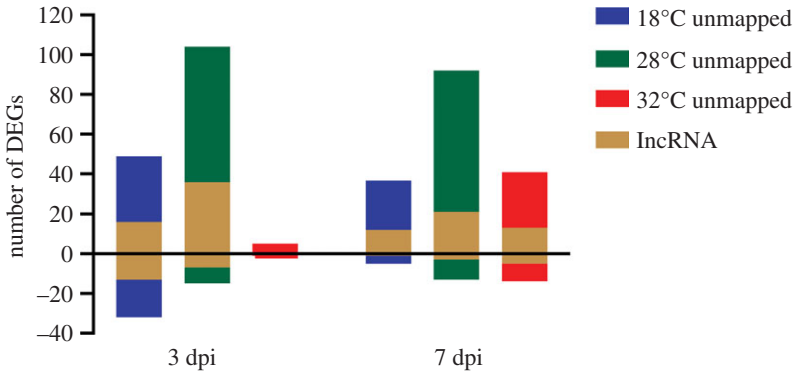

Figure 8. Number of differentially expressed genes (DEGs) that could not be mapped with DAVID bioinformatics cloud map. The number of lncRNA genes is shown within the total DEGs.

immune response is the recognition of pathogens by pattern recognition receptors [41]. Similar to previous studies [16,35,40,42], we identified diverse PRR genes being differentially expressed in our study, including CLIP-domain serine protease family B, FREP, LRR, leucine-rich transmembrane proteins, CTLs, TEP and galectins. However, we did not find any PRR DEGs common across all temperature treatments at 3 dpi, while at 7 dpi only *CLIPD6* was shared. There were no immune signalling or pathogen destruction-related genes found at the higher temperature (32°C), in contrast to the mosquitoes held at 28°C at both time points, which showed extensive upregulation of genes in both categories. Mosquitoes held at 18°C and 28°C showed significant upregulation of *Dicer-2*, critical in antiviral defence in *Aedes* spp. Mosquitoes [43], but there was no differential expression of this at 32°C. We observed additional immune genes become expressed at 32°C at 7 dpi as compared with 3 dpi, however this involved far fewer genes than at 28°C and *Dicer-2* was not differentially expressed. A limitation of our study is that we cannot rule out the presence of increased RNAi (*Dicer-2*) response immediately post infection (i.e. within 24 h), since our earliest time point was 3 dpi. Taken together, overall, our data suggest that the immune response to CHIKV is robust at 28°C, but key components fail to be activated at higher temperatures.

Complementing the strong immune response observed at 28°C, comprising Toll, IMD and JAK-STAT pathway components and *Dicer-2* activity, analysis on non-classical components of immunity revealed the doubling of Cytochrome P450 and serine protease gene numbers from 3 to 7 dpi in response to CHIKV infection. Cytochromes are generally involved in cellular functions including oxidative stress, respiration, apoptosis and xenobiotic metabolism [44]. The involvement of Cytochrome P450 in midguts of *Ae. aegypti* in response to DENV has been previously reported [45]. Increases in number of genes coding for serine proteases have also been reported for *Ae. aegypti* during DENV infection [46], thought to activate immune pathways through the triggering of serine protease cascades [47]. However, serine proteases may also aid arbovirus infection through proteolysis of extracellular matrix proteins, facilitating viral attachment [48]. Despite these strong immune defences at 28°C, we still observed an increase in CHIKV replication over time.

In our study, the highest number of downregulated genes was found at 18°C at 3 dpi. Experiments on *Drosophila* indicate that exposure to non-optimal/stressful low or high temperatures causes a significant reduction of lipid storage [49]. At low temperatures, there are reduced energy reserves owing to the slow accumulation of fat triggered by impaired biochemical activities. The lowering of metabolic rates may lead to a slowdown in the biosynthesis of key host resources necessary to the virus life cycle, resulting in reduced CHIKV replication. Consistent with this, we also observed downregulation of genes responsible for nucleic acid binding, indicating disturbance to gene regulation [50] and downregulation of the heterotrimeric G protein gene, which serves as a molecular switch to transduce stimuli from cell surface receptors into cells [51]. Additionally, fatty acid synthase (FAS), which is a critical enzyme in glycerophospholipid biosynthesis, was identified among topmost downregulated genes in these mosquitoes. A previous study indicated that inhibition of this enzyme enables mosquito cell survival but impairs dengue virus replication, as FAS is required in the viral replication cycle [52,53]. Therefore, at low temperatures, downregulation of FAS could also be antagonistic to CHIKV replication.

Mosquitoes have evolved various strategies to cope with different thermal conditions such as acclimation, adjusting behavioural activity and synthesis of heat shock proteins [54–56]. The downregulation at 32°C and 7 dpi of two sensory genes, namely odorant binding protein and long wavelength opsin, suggest a possible effect on mediators of behavioural activity. Insect long wavelength opsins have previously been implicated in insect thermoregulatory responses [57]. Production of HSP proteins such as HSP70 and small HSPs can result in more robust activation of insect defence mechanisms, and insect cells against mechanical and chemical stresses caused by damage to host tissue by invading pathogens [57–59]. Accordingly, we found significantly upregulated *hsp*70 gene expression in response to CHIKV infection across all temperatures in our study. Acclimation to cold temperatures also leads to elevation in HSP production [60]. Consistent with this, we found that the highest number of *hsp*70 genes expressed at 18°C, particularly at 3 dpi. It is worth noting that a member (*l2efl*) of the small heat shock protein *hsp*20 family, which has been suggested to suppress virus entry and interact with viral proteins [61], was in the top 10 upregulated genes across all temperatures and time points in our study. This is the first time, to our knowledge, that *hsp*20 involvement has been identified in *Ae. aegypti* in response to CHIKV infection, and may be specific to this interaction, as it has not been reportedly widely during arbovirus infection of mosquitoes.

We provide an updated list of genes involved in immune response, based on the most recent genome annotation of

Ae. aegypti. Previous studies of transcriptomic changes may be hampered by limited annotation and minimal literature on how immune genes/gene nomenclatures have changed [26] from the *Ae. aegypti* reference genome assembly version AaegL1 released in 2007 [62] to the AaegL5.2 version published in 2019 [29,30]. A limitation of our experiment is that we cannot rule out the influence of blood meal digestion in DEG patterns observed at 3 dpi. Although digestion may be completed by 3 dpi at the higher temperatures, at 18°C it may take longer than 3 days due to a slowdown in metabolism. Consistent with this, we observed significant downregulation of a zinc carboxypeptidase (AAEL008609) involved in blood meal digestion [63], suggesting lower temperature could disturb this process. This could slow down pathogen transmission because virus replication relies heavily on the availability of host resources [39,64].

We identified upregulation of genes related to pathways that facilitate viral transmission including glycerolipid metabolism, glycerophospholipid metabolism, ether lipid metabolism and sphingolipid metabolism which are known to facilitate DENV transmission by *Ae. aegypti* [65]. On the other hand, we saw downregulation of genes involved in DNA replication among topmost DEGs at 28°C, while GO analysis revealed a downregulation of cell proliferation genes at 3 dpi. A previous study performed using DENV-infected *Ae. aegypti* suggested that prevention of endoreplication of midgut cells enables the survival of the virus through the notch signalling pathway and leads to higher viral loads [66]. Our study is consistent with this, suggesting that downregulation of cell proliferation (and inhibition of DNA synthesis capacity [66]) may be beneficial to CHIKV replication.

Overall, our data suggest that temperature strongly influences the ability of mosquitoes to transmit viruses and the immune response during infection. At lower temperatures, downregulation of genes and conservation of resources may drive the viral replication observed despite the activation of many classical and non-classical immune components. A previous study identified a considerably higher number of differentially expressed genes between ZIKV infected and control mosquitoes at 20°C [18] compared with our findings. On the other hand, our study suggests that at high temperatures, the impairment of immune responses may result in shorter virus extrinsic incubation periods and higher virus titres. However, this response was not seen observed for ZIKV at 36°C in the previous study [18]. Impaired mosquito defences may result in a greater propensity for viruses to emerge in a warming climate. Conversely, impairment may also impose additional strong selection pressure on mosquitoes at high temperatures, resulting in altered behaviour and geographical ranges.

A final important observation is that time matters when dissecting response to infection, as varying repertoires of genes may be expressed at different points. A previous study using Zika virus-infected *Ae. aegypti* also identified time-dependent responses to gene expression during the early phase of infection, with differences observed at 24 and 48 h post infection [18]. Our data challenge the assumption that response to infection is constant through time in persistently infected mosquitoes. There was a 10-fold decrease from 3 dpi to 7 dpi in the number of downregulated genes in the number of DEGs observed at 18°C. Conversely, a 6.5-fold increase in the number of upregulated DEGs was observed at 32°C. The number of DEGs at 28°C remained more or less constant across time points but different repertoires of genes were expressed. In parallel, gene ontologies identified, and pathways enriched at these temperatures also differed.

A caveat of our study is that we were only able to examine six biological replicates for each experimental condition, the minimum recommended number for RNAseq experiments [67]. While many authors use pooled samples either due to financial or methodological (e.g. low RNA yields) concerns, a strength of our approach is that reveals individual biological variance [68]. However, additional insights may have been gained with the use of larger sample sizes.

In conclusion, we show that ambient temperature influences overall gene expression in response to CHIKV infection and suggest that high temperatures may impair mosquito immune response. Impaired mosquito responses may accelerate transmission of arboviruses and, potentially, pathogen emergence. The presence of a considerable number of lncRNA, pseudogenes and uncharacterized genes significantly differentially expressed in infected mosquitoes highlights the need for further functional studies and annotation of *Ae. aegypti* genome.

4. Methods

4.1. Mosquitoes and virus infection

Five- to 7-day old *Ae. aegypti* were orally challenged with virus-infected or sheep blood alone (control), using methods previously described [13]. A CHIKV strain from the Asian genotype (GenBank ID: MF773560) was prepared as described in [13] and delivered in oral feeds at a final pfu of 1×10^7 per ml of virus stock. Post oral challenge, mosquitoes observed to have taken a blood meal were randomly allocated to three different temperatures (18°C, 28°C and 32°C) in environmental chambers, with 70% humidity at a 12 h : 12 h day/night cycle. Mosquitoes were then sampled at 3 and 7 post infection. Mosquitoes were tested for the presence of CHIKV in whole bodies (minus wings and legs) using qRT-PCR as previously described [13].

4.2. RNA extraction and NGS sequencing

RNA was extracted from individual mosquito bodies using TRIzol reagent (Invitrogen, Thermo Fisher Scientific, USA). Samples were homogenized for 90 s with the addition of silica glass beads (Daintree Scientific, St Helens, TAS, Australia) in a MiniBeadbeater-96 (Biospec Products, Bartlesville, Oklahoma, USA). Total RNA was extracted from the homogenate according to the Trizol protocol. RNA was dissolved in Ultrapure water (Invitrogen, Thermo Fisher Scientific, USA) to make a final volume of 40 µl, and frozen at −80°C until further analysis.

4.3. Sample selection and RNAseq

Six mosquito bodies in which we detected the presence of CHIKV were selected from each time point, for each temperature. The samples were checked for RNA quality > 1.8 of A260/280 ratio and quantity by NanoDrop Lite (Thermo Fisher Scientific Inc.). RNA integrity was checked using RIN score analysis performed in an Agilent 2100 Bioanalyzer (Agilent Technologies, Palo Alto, CA, USA). Similarly, RNA extracted from uninfected control mosquitoes was subjected to quality and quantity checking. A total of 72 RNA samples,

comprising 36 infected blood-fed and 36 uninfected blood-fed controls were subjected to RNAseq, with six per each combination of time point (3 dpi and 7 dpi), and temperature (18, 28 and 32°C). Samples were sequenced on the Illumina HiSeq platform at Genewiz, China. Illumina raw data generated for all samples were deposited at the Short Read Archive (SRA) database under the BioProject accession number PRJNA630779.

4.4. RNAseq data analysis

Sequencing data obtained from Genewiz, China were subjected to quality control and mapping. Raw sequences in fastq format were subjected to adapter removal and quality trimming using Trim Galore (https://github.com/FelixKrueger/TrimGalore). Poor quality bases/reads with a quality score lower than 30 and sequences with a read length shorter than 50 nucleotides were removed to obtain high-quality clean data. To map the sequences, we first downloaded the reference genome sequences and annotations of AaegL5.2 from VectorBase (AaegL5) [29], the most recent annotation release of *Ae. aegypti* genome at the time of the analysis [30]. Second, RNA STAR two-pass mapping approach was used to align clean reads onto the AaegL5 reference genome sequence and obtain gene read counts [69]. The RSEM tool was then used to quantify the expression of gene isoforms [70]. Additionally, the RASflow pipeline [71] was used to align quality trimmed reads for individual samples onto the reference AaegL5.2 genome assembly. Differentially expressed genes (FDR < 0.05) were identified using DESeq2, an in-built module within the RASflow data analysis pipeline.

4.5. DEG identification, GO mapping and KEGG pathway analysis

Differential expression analysis was performed using the DESeq2 Bioconductor package [72]. The comparison between the mapped read counts of the virus-infected mosquitoes versus the read counts of uninfected blood-fed mosquitoes identified differentially expressed genes (DEGs). Genes were significantly differentially expressed if the adjusted *p*-value (false discovery rate) was < 0.05 and showed an absolute fold change of ±1.5. For all DEGs, gene annotation was done using the Biomart tool provided by the VectorBase database. DEG lists were further used for GO, pathway enrichment and immune response analysis. DAVID bioinformatics (V6.8) was used to assign GO terms and KEGG pathways information to differentially expressed genes [73]. WEGO 2.0 was then used to compare and plot GO annotation results at user-specified hierarchical level 2 [74]. The KEGG pathways enriched by DAVID bioinformatics were manually categorized under six main categories and subcategories as defined by the KEGG pathway database [75]. There were some pathways/GO terms with the presence of both up and downregulated genes. This is expected when pathways encode both positive and negative regulators [76]. Thus, if the upregulated gene group contains 'positive' regulators and downregulated one includes 'negative' regulators, in general, the pathway can be considered as regulated [76]. We used this approach in our descriptions of GO analysis and KEGG pathway analysis. For gene IDs for which functional information could not be assigned via DAVID bioinformatics (v6.8) gene enrichment analysis tool, then such genes were subjected to annotation using VectorBase search and BLAST sequence similarity (https://blast.ncbi.nlm.nih.gov/Blast.cgi).

4.6. Identification of classical and non-classical immune genes

We downloaded the peptide sequences of all the immune genes listed at the database ImmunoDB (http://cegg.unige.ch/Insecta/immunodb), which possesses information on insect immune-related genes and gene families [33]. We performed a similarity search using blastp with the peptides given in VectorBase (https://www.vectorbase.org/) under the annotation release AaegL5. Using an in-house script, we obtained the 10 best hits for each peptide and then selected the top hit with the largest bit score, percentage identity and lowest E-value. Next, we further searched the literature for articles using the search terms '*Aedes aegypti*' and 'immune' published after 2007 to ensure that we identify novel gene families/genes, that is, the genes recently discovered to link with immune response and thereby not covered in 2007 annotation of *Ae. aegypti*. In addition, a manual search for immune-related gene families/genes identified VectorBase annotated genes using previously identified gene family names. Genes that were related to four main categories of immune response process were considered classical immune genes while the genes directly or indirectly supplementing the above four processes are regarded as non-classical immune genes. The list of DEGs were compared against the list of immune genes identified through both literature review and similarity screening using Venny 2.1. Additionally, a list of lncRNA was identified comparing conserved ID sets between AaegL3.1 and AaegL5.1 gene annotation, and by including lncRNAs reported in AaegL5.2 [77].

4.7. CHIKV read count analysis

Estimation of chikungunya virus replication in infected and control *Ae. aegypti* was also performed by mapping high-quality adaptor-clipped Illumina pair-end reads onto the chikungunya virus genome, Asian genotype (GenBank accession no. MF773560) using Burrows-Wheeler Aligner (BWA) mem (https://arxiv.org/abs/1303.3997). Read counts of aligned reads were obtained using samtools idxstats [78]. Normalized reads per million (RPM) counts were calculated to quantify viral read counts. Two samples (RY-74 and RY-75) were identified as outliers on the correlation plot between virus titre and normalized reads per million counts and were removed from further analysis. The Mann–Whitney test was used to find differences between virus read counts of any two mosquito groups. The Kruskal–Wallis test was used for comparison of viral reads of multiple groups. A *p*-value < 0.05 was considered statistically significant. Statistical analyses were performed using SPSS 25 (IBM Statistics). Graphs were prepared using GraphPad Prism version 8.3.0.

Data accessibility. The data were deposited at NCBI's Short Read Archive (SRA) database under the BioProject accession number PRJNA630779.

Authors' contributions. B.M.C.R.W.-Y. performed molecular and experimental laboratory work, data analysis, and writing and editing of the manuscript; R.A.B. performed data analysis and writing and editing of the paper; L.S. performed molecular and experimental laboratory work, and editing of the manuscript; L.M.H. supervised analysis and critically revised the manuscript; E.A.M. provided input into the design of the study and analysis, critically revised the manuscript and contributed to securing funding for the research; A.T.P.

provided experimental reagents and critically revised the manuscript; C.C.J. provided input into the design of the study and analysis, and critically revised the manuscript; A.S. provided input into the analysis, and critically revised the manuscript; L.Y. provided input into the design of the study and analysis, critically revised the manuscript and contributed to securing funding for the research; W.H. provided input into the design of the study and analysis, critically revised the manuscript and contributed to securing funding for the research; G.J.D. provided input into the design of the study and analysis, critically revised the manuscript and contributed to securing funding for the research; F.D.F. conceived the study, provided input into the design and analysis of the study, critically revised the manuscript, supervised experiments and secured funding for research.

Competing interests. We declare we have no competing interests.

Funding. The research presented here was funded by the National Health and Medical Research Council (NHMRC) of Australia project grant no. APP1125317 and the Royal Society of Tropical Medicine and Hygiene small grants program. B.M.C.R.W.-Y. was funded by the University Grants Commission Sri Lanka, the Open University of Sri Lanka and QUT.

Acknowledgements. We thank Mr Henry Simila for technical assistance and the Research Methods Group in the Institute for Health and Biomedical Innovation (IHBI), Queensland University of Technology (QUT), Brisbane, Australia, for statistical advice. We also thank the anonymous reviewers whose comments greatly improved the manuscript. Last, we thank Dr Chen Wu for the original mosquito photo that inspired the image accompanying this article and Mr David van der Heide for graphic design advice.

References

1. World Health Organization. 2014 *A global brief on vector-borne diseases*. Geneva, Switzerland: World Health Organization.
2. Forshey BM *et al*. 2010 Arboviral etiologies of acute febrile illnesses in Western South America, 2000–2007. *PLoS Negl. Trop. Dis.* **4**, e787.
3. Caminade C, McIntyre KM, Jones AE. 2019 Impact of recent and future climate change on vector-borne diseases. *Ann. NY Acad. Sci.* **1436**, 157–173. (doi:10.1111/nyas.13950)
4. Shapiro LLM, Whitehead SA, Thomas MB. 2017 Quantifying the effects of temperature on mosquito and parasite traits that determine the transmission potential of human malaria. *PLoS Biol.* **15**, e2003489. (doi:10.1371/journal.pbio.2003489)
5. Huang X, Hu W, Yakob L, Devine GJ, McGraw EA, Jansen CC, Faddy HM, Frentiu FD. 2019 El Niño Southern oscillation, overseas arrivals and imported chikungunya cases in Australia: a time series analysis. *PLoS Negl. Trop. Dis.* **13**, e0007376. (doi:10.1371/journal.pntd.0007376)
6. Iwamura T, Guzman-Holst A, Murray KA. 2020 Accelerating invasion potential of disease vector *Aedes aegypti* under climate change. *Nat. Commun.* **11**, 2130. (doi:10.1038/s41467-020-16010-4)
7. Kraemer MUG *et al*. 2019 Past and future spread of the arbovirus vectors *Aedes aegypti* and *Aedes albopictus*. *Nat. Microbiol.* **4**, 854–863. (doi:10.1038/s41564-019-0376-y)
8. Messina JP *et al*. 2019 The current and future global distribution and population at risk of dengue. *Nat. Microbiol.* **4**, 1508–1515. (doi:10.1038/s41564-019-0476-8)
9. Xu Z, Bambrick H, Frentiu FD, Devine GJ, Yakob L, Williams G, Hu W. 2020 Projecting the future of dengue under climate change scenarios: progress, uncertainties and research needs. *PLoS Negl. Trop. Dis.* **14**, e0008118. (doi:10.1371/journal.pntd.0008118)
10. Alto BW, Bettinardi D. 2013 Temperature and dengue virus infection in mosquitoes: independent effects on the immature and adult stages. *Amer. J. Trop. Med. Hyg.* **88**, 497–505. (doi:10.4269/ajtmh.12-0421)
11. Watts DM, Burke DS, Harrison BA, Whitmire RE, Nisalak A. 1987 Effect of temperature on the vector efficiency of *Aedes aegypti* for dengue 2 virus. *Amer. J. Trop. Med. Hyg.* **36**, 143–152. (doi:10.4269/ajtmh.1987.36.143)
12. Ciota AT, Keyel AC. 2019 The role of temperature in transmission of zoonotic arboviruses. *Viruses* **115**, 1013. (doi:10.3390/v11111013)
13. Wimalasiri-Yapa BMCR *et al*. 2019 Chikungunya virus transmission at low temperature by *Aedes albopictus* mosquitoes. *Pathogens* **8**, 149. (doi:10.3390/pathogens8030149)
14. Strand MR. 2008 The insect cellular immune response. *Insect Science* **15**, 1–14. (doi:10.1111/j.1744-7917.2008.00183.x)
15. Hillyer JF. 2016 Insect immunology and hematopoiesis. *Dev. Comp. Immunol.* **58**, 102–118. (doi:10.1016/j.dci.2015.12.006)
16. Etebari K, Hegde S, Saldaña MA, Widen SG, Wood TG, Asgari S, Fernandez-Sesma A. 2017 Global transcriptome analysis of *Aedes aegypti* mosquitoes in response to zika virus infection. *mSphere* **2**, e00456-17. (doi:10.1128/mSphere.00456-17)
17. Etebari K, Asad S, Zhang G, Asgari S. 2016 Identification of *Aedes aegypti* long intergenic non-coding RNAs and their association with *Wolbachia* and dengue virus infection. *PLoS Negl. Trop. Dis.* **105**, e0005069. (doi:10.1371/journal.pntd.0005069)
18. Ferreira PG, Tesla B, Horácio ECA, Nahum LA, Brindley MA, de Oliveira TAM. 2020 Temperature dramatically shapes mosquito gene expression with consequences for mosquito–Zika virus interactions. *Front. Microbiol.* **11**, 901. (doi:10.3389/fmicb.2020.00901)
19. Furuya-Kanamori L *et al*. 2016 Co-distribution and co-infection of chikungunya and dengue viruses. *BMC Infect. Dis.* **16**, 84. (doi:10.1186/s12879-016-1417-2)
20. Suhrbier A. 2019 Rheumatic manifestations of chikungunya: emerging concepts and interventions. *Nat. Rev. Rheumatol.* **155**, 597–611. (doi:10.1038/s41584-019-0276-9)
21. Wimalasiri-Yapa BMCR *et al*. 2019 Chikungunya virus in Asia-Pacific: a systematic review. *Emerg. Microbes Infect.* **8**, 70–79. (doi:10.1080/22221751.2018.1559708)
22. Lumsden WHR. 1955 An epidemic of virus disease in Southern Province, Tanganyika Territory, in 1952–53. I. Clinical features. *Trans. R. Soc. Trop. Med. Hyg.* **49**, 28. (doi:10.1016/0035-9203(55)90080-8)
23. Tsetsarkin KA, Vanlandingham DL, McGee CE, Higgs S. 2007 A single mutation in chikungunya virus affects vector specificity and epidemic potential. *PLoS Pathog.* **3**, e201. (doi:10.1371/journal.ppat.0030201)
24. Staples JE, Hills SL, Powers AM. 2020 Chikungunya. In *CDC yellow book*. See wwwnc.cdc.gov/travel/yellowbook/2020/travel-related-infectious-diseases/chikungunya.
25. World Health Organization. 2020 Dengue and severe dengue 2020. See https://www.who.int/news-room/fact-sheets/detail/dengue-and-severe-dengue
26. Adelman ZN, Myles KM. 2018 The C-type lectin domain gene family in *Aedes aegypti* and their role in arbovirus infection. *Viruses*. **10**, 367. (doi:10.3390/v10070367)
27. Bonizzoni M *et al*. 2011 RNA-seq analyses of blood-induced changes in gene expression in the mosquito vector species, *Aedes aegypti*. *BMC Genomics* **12**, 82. (doi:10.1186/1471-2164-12-82)
28. Gross TL, Myles KM, Adelman ZN. 2009 Identification and characterization of heat shock 70 genes in *Aedes aegypti* (Diptera: Culicidae). *J. Med. Entomol.* **46**, 496–504. (doi:10.1603/033.046.0313)
29. Lawson D *et al*. 2008 VectorBase: a data resource for invertebrate vector genomics. *Nucleic Acids Res.* **37**(Suppl_1), D583–D587.
30. Matthews BJ *et al*. 2018 Improved reference genome of *Aedes aegypti* informs arbovirus vector control. *Nature* **563**, 501–507. (doi:10.1038/s41586-018-0692-z)
31. Wang J, Song X, Wang M. 2018 Peptidoglycan recognition proteins in hematophagous arthropods. *Dev. Comp. Immunol.* **83**, 89–95. (doi:10.1016/j.dci.2017.12.017)
32. Wang YH, Chang MM, Wang XL, Zheng AH, Zou Z. 2018 The immune strategies of mosquito *Aedes aegypti* against microbial infection. *Dev. Comp. Immunol.* **83**, 12–21. (doi:10.1016/j.dci.2017.12.001)
33. Waterhouse RM *et al*. 2007 Evolutionary dynamics of immune-related genes and pathways in disease-vector mosquitoes. *Science* **316**, 1738–1743. (doi:10.1126/science.1139862)
34. Xiao X, Liu Y, Zhang X, Wang J, Li Z, Pang X, Wang P, Cheng G. 2014 Complement-related proteins control the flavivirus infection of *Aedes aegypti* by inducing antimicrobial peptides. *PLoS*

Pathog. **10**, e1004027. (doi:10.1371/journal.ppat.1004027)

35. Zhao L, Alto BW, Jiang Y, Yu F, Zhang Y. 2019 Transcriptomic analysis of *Aedes aegypti* innate immune system in response to ingestion of chikungunya virus. *Int. J. Mol. Sci.* **205**, 3133. (doi:10.3390/ijms20133133)
36. Lee W-S, Webster JA, Madzokere ET, Stephenson EB, Herrero LJ. 2019 Mosquito antiviral defense mechanisms: a delicate balance between innate immunity and persistent viral infection. *Parasit. Vectors* **12**, 165. (doi:10.1186/s13071-019-3433-8)
37. Sigle LT, McGraw EA. 2019 Expanding the canon: non-classical mosquito genes at the interface of arboviral infection. *Insect Biochem. Mol. Biol.* **109**, 72–80. (doi:10.1016/j.ibmb.2019.04.004)
38. Dillon ME, Wang G, Huey RB. 2010 Global metabolic impacts of recent climate warming. *Nature* **467**, 704–706. (doi:10.1038/nature09407)
39. Heaton NS, Perera R, Berger KL, Khadka S, LaCount DJ, Kuhn RJ, Randall G. 2010 Dengue virus nonstructural protein 3 redistributes fatty acid synthase to sites of viral replication and increases cellular fatty acid synthesis. *Proc. Natl Acad. Sci. USA* **1075**, 17 345–17 350. (doi:10.1073/pnas.1010811107)
40. Colpitts TM *et al*. 2011 Alterations in the *Aedes aegypti* transcriptome during infection with west Nile, dengue and yellow fever viruses. *PLoS Pathog.* **7**, e1002189. (doi:10.1371/journal.ppat.1002189)
41. Kingsolver MB, Huang Z, Hardy RW. 2013 Insect antiviral innate immunity: pathways, effectors, and connections. *J. Mol. Biol.* **4255**, 4921–4936. (doi:10.1016/j.jmb.2013.10.006)
42. Dong S, Behura SK, Franz AWE. 2017 The midgut transcriptome of *Aedes aegypti* fed with saline or protein meals containing chikungunya virus reveals genes potentially involved in viral midgut escape. *BMC Genomics* **18**, 382. (doi:10.1186/s12864-017-3775-6)
43. Sabin LR *et al*. 2013 Dicer-2 processes diverse viral RNA species. *PLoS ONE* **8**, e55458. (doi:10.1371/journal.pone.0055458)
44. Scott JG, Kasai S. 2004 Evolutionary plasticity of monooxygenase-mediated resistance. *Pestic Biochem. Phys.* **78**, 171–178. (doi:10.1016/j.pestbp.2004.01.002)
45. Barón OL, Ursic-Bedoya RJ, Lowenberger CA, Campo CB. 2010 Differential gene expression from midguts of refractory and susceptible lines of the mosquito, *Aedes aegypti*, infected with dengue-2 virus. *J. Insect Sci.* **10**. (doi:10.1673/031.010.4101)
46. Bonizzoni M, Dunn WA, Campbell CL, Olson KE, Marinotti O, James AA. 2012 Complex modulation of the *Aedes aegypti* transcriptome in response to Dengue virus infection. *PLoS ONE* **75**, e50512. (doi:10.1371/journal.pone.0050512)
47. Brackney DE, Foy BD, Olson KE. 2008 The effects of midgut serine proteases on dengue virus type 2 infectivity of *Aedes aegypti*. *Am. J. Trop. Med. Hyg.* **79**, 267–274. (doi:10.4269/ajtmh.2008.79.267)
48. Conway MJ *et al*. 2014 Mosquito saliva serine protease enhances dissemination of dengue virus into the mammalian host. *J. Virol.* **88**, 164–175. (doi:10.1128/JVI.02235-13)
49. Klepsatel P, Wildridge D, Gáliková M. 2019 Temperature induces changes in *Drosophila* energy stores. *Sci. Rep.* **9**, 5239. (doi:10.1038/s41598-019-41754-5)
50. Laity JH, Lee BM, Wright PE. 2001 Zinc finger proteins: new insights into structural and functional diversity. *Curr. Opin. Struct. Biol.* **11**, 39–46. (doi:10.1016/S0959-440X(00)00167-6)
51. Suzuki N, Hajicek N, Kozasa T. 2009 Regulation and physiological functions of G12/13-mediated signaling pathways. *Neurosignals* **17**, 55–70. (doi:10.1159/000186690)
52. Perera R *et al*. 2012 Dengue virus infection perturbs lipid homeostasis in infected mosquito cells. *PLoS Pathogens* **8**, e1002584. (doi:10.1371/journal.ppat.1002584)
53. Tongluan N *et al*. 2017 Involvement of fatty acid synthase in dengue virus infection. *Virol. J.* **14**, 1–8. (doi:10.1186/s12985-017-0685-9)
54. Benoit JB, Lopez-Martinez G, Patrick KR, Phillips ZP, Krause TB, Denlinger DL. 2011 Drinking a hot blood meal elicits a protective heat shock response in mosquitoes. *Proc. Natl Acad. Sci. USA* **1085**, 8026–8029. (doi:10.1073/pnas.1105195108)
55. Hanson SM, Craig Jr GB. 1994 Cold acclimation, diapause, and geographic origin affect cold hardiness in eggs of *Aedes albopictus* (Diptera: Culicidae). *J. Med. Entomol.* **31**, 192–201. (doi:10.1093/jmedent/31.2.192)
56. Jass A, Yerushalmi GY, Davis HE, Donini A, MacMillan HA. 2019 An impressive capacity for cold tolerance plasticity protects against ionoregulatory collapse in the disease vector, *Aedes aegypti*. *bioRxiv*, 745885.
57. Frentiu FD, Yuan F, Savage WK, Bernard GD, Mullen SP, Briscoe AD. 2015 Opsin clines in butterflies suggest novel roles for insect photopigments. *Mol. Biol. Evol.* **32**, 368–379. (doi:10.1093/molbev/msu304)
58. Merkling SH, Overheul GJ, van Mierlo JT, Arends D, Gilissen C, van Rij RP. 2015 The heat shock response restricts virus infection in *Drosophila*. *Sci. Rep.* **5**, 12758. (doi:10.1038/srep12758)
59. Wojda I. 2017 Temperature stress and insect immunity. *J. Therm. Biol.* **68**, 96–103. (doi:10.1016/j.jtherbio.2016.12.002)
60. Teigen LE, Orczewska JI, McLaughlin J, O'Brien KM. 2015 Cold acclimation increases levels of some heat shock protein and sirtuin isoforms in threespine stickleback. *Comp. Biochem. Physiol. A Mol. Integr. Physiol.* **188**, 139–147. (doi:10.1016/j.cbpa.2015.06.028)
61. Li J, Xiang C-Y, Yang J, Chen J-P, Zhang H-M. 2015 Interaction of HSP20 with a viral RdRp changes its sub-cellular localization and distribution pattern in plants. *Sci. Rep.* **5**, 14016. (doi:10.1038/srep14016)
62. Nene V *et al*. 2007 Genome sequence of *Aedes aegypti*, a major arbovirus vector. *Science* **316**, 1718–1723. (doi:10.1126/science.1138878)
63. Isoe J, Zamora J, Miesfeld RL. 2009 Molecular analysis of the *Aedes aegypti* carboxypeptidase gene family. *Insect Biochem. Mol. Biol.* **39**, 68–73. (doi:10.1016/j.ibmb.2008.09.006)
64. Rampersad S, Tennant P. 2018 Replication and expression strategies of viruses. In *Viruses: molecular biology, host interactions and applications to biotechnology* (eds P Tennant, G Fermin, JE Foster), pp. 55–82. Oxford, UK: Elsevier
65. Chotiwan N *et al*. 2018 Dynamic remodeling of lipids coincides with dengue virus replication in the midgut of *Aedes aegypti* mosquitoes. *PLoS Pathogens* **14**, e1006853. (doi:10.1371/journal.ppat.1006853)
66. Serrato-Salas J, Hernández-Martínez S, Martínez-Barnetche J, Condé R, Alvarado-Delgado A, Zumaya-Estrada F, Lanz-Mendoza H. 2018 De novo DNA synthesis in *Aedes aegypti* midgut cells as a complementary strategy to limit dengue viral replication. *Front. Microbiol.* **9**, 801. (doi:10.3389/fmicb.2018.00801)
67. Schurch NJ *et al*. 2016 How many biological replicates are needed in an RNA-seq experiment and which differential expression tool should you use? *RNA* **22**, 839–851. (doi:10.1261/rna.053959.115)
68. Zhang S-D, Gant TW. 2005 Effect of pooling samples on the efficiency of comparative studies using microarrays. *Bioinformatics* **215**, 4378–4383. (doi:10.1093/bioinformatics/bti717)
69. Dobin A, Davis CA, Schlesinger F, Drenkow J, Zaleski C, Jha S, Batut P, Chaisson M, Gingeras TR. 2013 STAR: ultrafast universal RNA-seq aligner. *Bioinformatics* **29**, 15–21. (doi:10.1093/bioinformatics/bts635)
70. Li B, Dewey CN. 2011 RSEM: accurate transcript quantification from RNA-Seq data with or without a reference genome. *BMC Bioinformatics* **12**, 323. (doi:10.1186/1471-2105-12-323)
71. Zhang X, Jonassen I. 2020 RASflow: an RNA-Seq analysis workflow with Snakemake. *BMC Bioinformatics* **21**, 110. (doi:10.1186/s12859-020-3433-x)
72. Love MI, Huber W, Anders S. 2014 Moderated estimation of fold change and dispersion for RNA-seq data with DESeq2. *Genome Biol.* **155**, 550. (doi:10.1186/s13059-014-0550-8)
73. Sherman BT *et al*. 2007 The DAVID gene functional classification tool: a novel biological module-centric algorithm to functionally analyze large gene lists. *Genome Biol.* **8**, R183. (doi:10.1186/gb-2007-8-9-r183)
74. Ye J *et al*. 2018 WEGO 2.0: a web tool for analyzing and plotting GO annotations, 2018 update. *Nucleic Acids Res.* **46**, W71–W75. (doi:10.1093/nar/gky400)
75. Kanehisa M, Goto S. 2000 KEGG: kyoto encyclopedia of genes and genomes. *Nucleic Acids Res.* **28**, 27–30. (doi:10.1093/nar/28.1.27)
76. Warden CD, Kanaya N, Chen S, Yuan Y-C. 2013 BD-Func: a streamlined algorithm for predicting activation and inhibition of pathways. *PeerJ.* **1**, e159. (doi:10.7717/peerj.159)
77. Azlan A, Obeidat SM, Yunus MA, Azzam G. 2019 Systematic identification and characterization of *Aedes aegypti* long noncoding RNAs (lncRNAs). *Sci. Rep.* **9**, 12147. (doi:10.1038/s41598-019-47506-9)
78. Li H *et al*. 2009 The sequence alignment/map format and SAMtools. *Bioinformatics* **255**, 2078–2079. (doi:10.1093/bioinformatics/btp352)